Science of the Total Environment 473–474 (2014) 381–390

Contents lists available at ScienceDirect

Science of the Total Environment

journal homepage: www.elsevier.com/locate/scitotenv

Dynamics of suspended sediment borne persistent organic pollutants in a large regulated Mediterranean river (Ebro, NE Spain)

S. Quesada [a], A. Tena [b], D. Guillén [a], A. Ginebreda [a,*], D. Vericat [b,d,e], E. Martínez [a], A. Navarro-Ortega [a], R.J. Batalla [b,c,d], D. Barceló [a,c]

[a] Department of Environmental Chemistry, IDAEA-CSIC, c/Jordi Girona 18-26, E-08034 Barcelona, Spain
[b] Department of Environment and Soil Sciences, University of Lleida, E-25198 Lleida, Spain
[c] Catalan Institute for Water Research (ICRA), Emili Grahit 101, E-17003 Girona, Spain
[d] Forest Technology Centre of Catalonia, E-25280 Solsona, Spain
[e] Institute of Geography and Earth Sciences, Aberystwyth University, Wales, Ceredigion SY23 3DB, UK

GRAPHICAL ABSTRACT

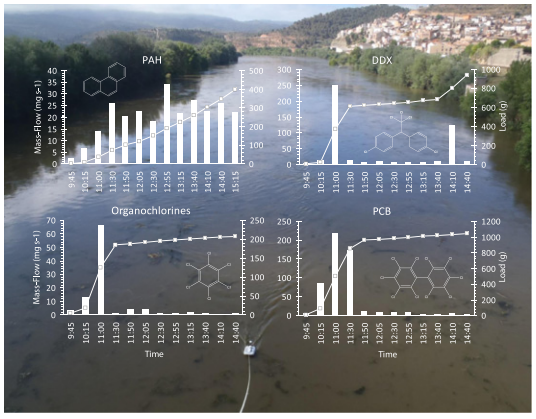

ARTICLE INFO

Article history:
Received 7 August 2013
Received in revised form 6 November 2013
Accepted 7 November 2013
Available online 28 December 2013

Keywords:
Suspended sediments
Persistent organic pollutants
Flushing flows
Pollutants' transport
Mass loads
River Ebro

ABSTRACT

Mediterranean rivers are characterized by highly variable hydrological regimes that are strongly dependent on the seasonal rainfall. Sediment transport is closely related to the occurrence of flash-floods capable to deliver enough kinetic energy to mobilize the bed and channel sediments. Contaminants accumulated in the sediments are likely to be mobilized as well during such events. However, whereas there are many studies characterizing contaminants in steady sediments, those devoted to the transport dynamics of suspended-sediment borne pollution are lacking. Here we examined the occurrence and transport of persistent organic microcontaminants present in the circulating suspended sediments during a controlled flushing flow in the low part of the River Ebro (NE Spain) 12 km downstream of a well-known contaminated hot-spot associated to a nearby chloro-alkali industry. Polycyclic aromatic hydrocarbons (PAHs) and semi-volatile organochlorine pollutants (DDT and related compounds, DDX; polychlorinated byphenils, PCBs; and other organochlorine compound, OCs) were measured in the particulate material by GC–MS and GC–MS/MS, using previously developed analytical

* Corresponding author. Tel.: +34 934006100.
E-mail address: antoni.ginebreda@idaea.csic.es (A. Ginebreda).

http://dx.doi.org/10.1016/j.scitotenv.2013.11.040

methods. The concentration levels observed were compared to previously reported values in steady sediments in the same river and discussed on a regulatory perspective. Hydrographs and sedigraphs recorded showed a peak-flow of 1300 $m^3\ s^{-1}$ and a corresponding peak of suspended sediments of 315 mg L^{-1}. Combination of flow discharge, suspended sediments and pollutants' concentrations data allowed for quantifying the mass flows (mass per unit of time) and setting the load budgets (weight amount) of the different pollutants transported by the river during the monitored event. Mean mass-flows and total load values found were 20.2 mg s^{-1} (400 g) for PAHs, 38 mg s^{-1} (940 g) for DDX, 44 mg s^{-1} (1038 g) for PCBs and 8 mg s^{-1} (200 g) for OCs. The dynamic pattern behavior of PAHs differs substantially to that of organochlorine pollutants, thus reflecting different pollution origins.

1. Introduction

Water scarcity is present in natural conditions in the Mediterranean area due to the characteristic highly variable river flows and the occurrence of low flow characteristic of the Mediterranean climate. Alternation of extreme events such as droughts and flash-floods is common in the region, a fact that will likely accentuate according to the previsions of the IPCC (Lehner et al., 2006). Sediment transport is closely related to the occurrence of flood events (Batalla et al., 1995; Garcia et al., 2000; Vericat and Batalla, 2010) capable to deliver enough kinetic energy to mobilize the riverbed and entrain the sediments. Likewise, it is known that contaminants accumulated in the sediments are mobilized during such energetic events. However, whereas there are many studies characterizing contaminants in steady sediments (Fernández et al., 1999; Carrizo and Grimalt, 2006; Lacorte et al., 2006; Navarro-Ortega et al., 2010), only few are devoted specifically to the transport dynamics of pollutants associated to the suspended sediment load (Gómez-Gutiérrez et al., 2006). In addition, quantitative information concerning the load budgets of persistent organic pollutants associated to particulate material transport is scarce (Schwientek et al., 2013; Rügner et al., 2013). Within this context, flushing flows (FF), which are controlled flood flows performed from a dam for a given environmental and/or engineering purpose (Kondolf and Wilcock, 1996; Batalla and Vericat, 2009), offer some advantageous characteristics (in comparison to natural floods) to examine the role of the suspended loads in entraining and transporting associated contaminants. It has been shown that during FFs suspended sediment concentration doubles that of natural floods, although discharges are typically much lower (Tena et al., 2012b). In turn, flashiness, measured as the rate of discharge increment per unit time, may attain an order of magnitude higher during FFs than during natural events. Consequently, FFs exhibit higher transport capacity than their natural counterparts despite their considerably lower magnitude and duration. Furthermore, and owing to their intrinsic characteristics (i.e. hydrograph design, programmability), they offer obvious practical advantages, particularly in what monitoring logistics is concerned.

FFs have been used typically to mitigate dam-induced impacts, mobilizing accumulated sediment and scouring the channel (Milhous, 1982), and maintaining large morphological features (Reiser et al., 1989). Under appropriate conditions, they are increasingly used as a tool for the maintenance and enhancement of aquatic and riparian habitat (Brookes, 1995; Kondolf and Wilcock, 1996; Downs et al., 2002). In particular, FFs have been implemented in the lower Ebro River since 2002 and have been extensively monitored and subsequently analyzed, even modeled (Batalla and Vericat, 2009; Tena et al., 2011, 2012a, 2012b). In the present work, we examine the dynamics of persistent organic microcontaminants associated to the suspended sediments during a particular FF that was performed in the lower River Ebro (NE Spain) in June 2012. Measurements were taken 12 km downstream of a well-known contaminated hot-spot (Amaral et al., 1996; Olivares et al., 2010; Soto et al., 2011) associated to a nearby chloro-alkali industry (Flix) (Fig. 1).

A total of 42 semi-volatile persistent organic compounds corresponding to the families of polycyclic aromatic hydrocarbons (PAHs), DDT and its metabolites (DDX), polychlorinated biphenyls (PCBs) and other organochlorine compounds (OCs) were monitored. The objectives of the paper are (a) to analyze the presence of persistent organic pollutants associated to the suspended sediment load; (b) to characterize their variation during one of the artificial releases (flushing-flow) that are regularly performed in this river; (c) to provide a quantitative assessment of the mass-flows and load budgets of the organic microcontaminants transported during the FF; and (d) to assess the risk associated to such transport, also by putting the results in the current regulatory context.

2. Site description: The lower Ebro

The Ebro is the largest river in the Iberian Peninsula flowing into the Mediterranean Sea, with a basin draining a total of 85,534 km^2 (Fig. 1). It is characterized by an interannual variability associated with its intrinsic Mediterranean character. Mean discharge recorded in Tortosa (i.e. the lowermost downstream gauging station) for the period 1912–2012 is 436 $m^3\ s^{-1}$, but flows vary from less than 50 $m^3\ s^{-1}$ in the very dry seasons to more than 12,000 $m^3\ s^{-1}$ (i.e. the major flood recorded ever that occurred in October 1907 Novoa, 1984).

Runoff in the Ebro is regulated by a series of dams. In particular, in the lower Ebro (where we focus our study) the Mequinenza–Ribarroja–Flix dam complex is located; it owns a total storage capacity of ~1.7 km^3 (i.e. 1 $km^3 = 1 \times 10^9\ m^3$), the largest in the catchment. Regulation has led to a decrease of an average of 25% the magnitude of natural frequent floods (i.e. Q_2–Q_{25}, where Q_i is the discharge associated with i years recurrence interval) in the reach downstream the dams (Batalla et al., 2004). Sediment transfer has also been altered; for instance, Vericat and Batalla (2006) reported a mean trapping efficiency for suspended sediment at around 90% in the dam complex, whereas bedload is fully captured. Together with hydrological and sedimentological alterations because of regulation (Batalla et al., 2004; Vericat and Batalla, 2006; Tena et al., 2012a) ecological consequences have also been observed in the lowermost part of the catchment (Prats et al., 2011; Sabater et al., 2011); for instance, the massive growth of macrophytes (Batalla and Vericat, 2009; Tena et al., 2012a). Within this context, FFs have been designed and implemented in the lower Ebro since 2002 with a twofold objective: (i) controlling macrophyte populations and (ii) maintaining certain degree of sedimentary activity in the channel. However, river regulation is not the only impact in the lower Ebro. The Flix Reservoir is heavily affected by wastes from a chloro-alkali plant. The result of the accumulation of waste disposal from the factory through decades is a deposit of hazardous industrial solid waste (200,000–360,000 T) which contains large amounts of PCBs, DDT, hexachlorocyclohexane (HCB) and heavy metals (Hg) (Fernández et al., 1999). Today, this deposit is a major concern and decontamination works are being carried out. This decontamination involves the removal of the contaminated sludge of the river by dredging, a subsequent processing at a nearby treatment plant, transportation and disposal in landfill of contaminated wastes. Consequently, the present study can be used as a tool for the evaluation of the effects of this dredging process on the Ebro River downstream from Flix.

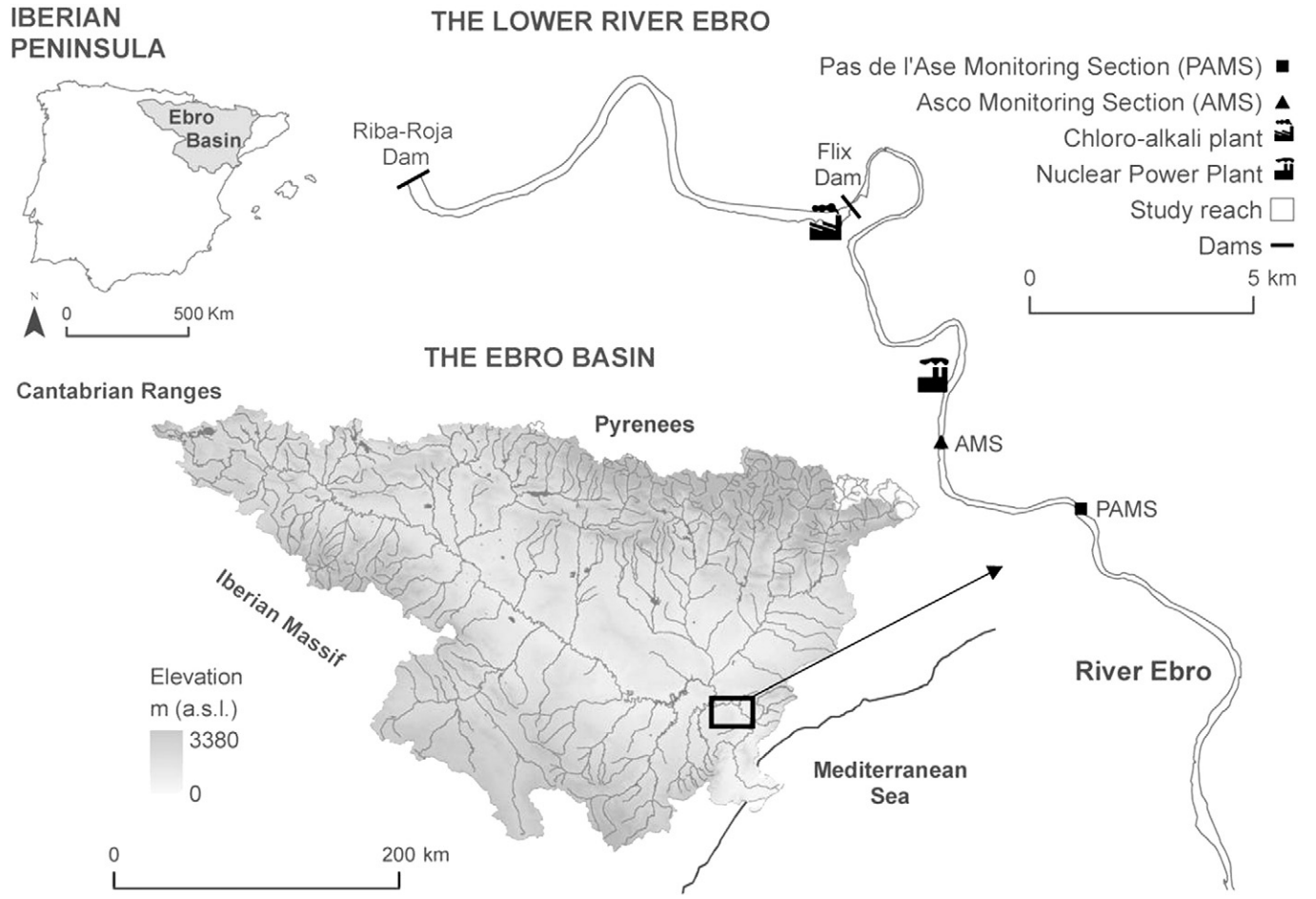

Fig. 1. The Ebro River basin with the location of the study area.

In order to examine the dynamics of the microcontaminants of concern during the June 2012 FF downstream Flix dam, two sampling sections were established: Ascó Monitoring Section (AMS), located 12 km downstream the dam and Pas de l'Ase Monitoring Section (PAMS), located 4 km downstream AMS and 16 km downstream the Flix dam (Fig. 1).

3. Methods

3.1. Flow monitoring

Flow and sediment transport were monitored at the two sections previously selected (AMS and PAMS) during the FF performed in June 2012. Data on water release from the dam complex was provided by the dam operator (Endesa Generación SA); moreover, discharge is routinely measured by Ebro Water Authorities (Confederación Hidrográfica del Ebro, CHE) at AMS (Fig. 1) (CHE, 2012; SAIH, 2012). There, water stage (h) is recorded every 15 min by an OTT Water Level and transformed into discharge (Q) using an ad-hoc calibrated h-Q rating curve. In order to corroborate the official CHE data calibration, discharge measurements were done by means of acoustic methods (i.e. ADCP River Surveyor M9®, Sontek) during the flood. The hydrograph at PAMS (located 4 km downstream from AMS) has been directly routed from AMS by means of the Muskingum method (Tena et al., 2011, 2012a).

3.2. Sampling of sediment and chemical loads

Suspended sediment concentrations (SSC, in mg L^{-1}) have been obtained from (i) direct sampling in AMS and (ii) indirect data (i.e. turbidity measurements) in PAMS: (i) Suspended sediments were sampled during the event by means of a cable-suspended bucket sampler at 30 min interval from the Ascó Bridge (200 meter upstream AMS). Sampling was carried out in a single vertical, in the midpoint of the transverse section of the river, according to (Vericat and Batalla, 2006). The resulting water samples were lately vacuum filtered at the laboratory by means of glass microfiber filters (Filter-Lab, 1.2 μm pore size), dried and weighed to determine SSC. The method reported by Tena et al. (2011) was followed to determine the organic matter content; then, the percentage of organic matter was subtracted from the filter weight to obtain the net particulate suspended sediment load.

(ii) Suspended sediment concentrations were also obtained by means of an indirect method: water turbidity, a proxy of suspended sediment, and was recorded every 15 min at the water quality station of PAMS by means of a Hach SS6 turbidity probe. Subsequently, turbidity series were calibrated with a total of 150 water samples already obtained during floods, and weekly or fortnightly during low flows (Tena and Batalla, 2013). A correlation between pair values of turbidity (in NTU; i.e. Nephelometric Turbidity Units) and SSC (mg L^{-1}) was established for the PAMS turbidity probe. The relation fitted to a linear regression ($SSC = 0.83 \times NTU - 1.3$) was then used to obtain the corresponding SSC values (Tena et al., 2011; Tena and Batalla, 2013) (see Fig. S1, Supporting material). The suspended sediment mass-flow transported during the FF was calculated by multiplying the hourly SSC (in mg L^{-1}) by Q (in m^3 s^{-1}).

In turn, water samples, specifically taken for the chemical analysis of the suspended sediments were also sampled during the flash-flood event from AMS using the methodology explained in (i). Each collected water sample was transferred to a 10 L polypropylene flask, labeled and stored in mobile refrigerators to be properly transported to the

laboratory. At the end of the sampling campaign a total of 13 water samples were collected intensively from 9:45 to 15:30 with frequencies between 15 and 30 min.

3.3. Chemical analysis

3.3.1. Chemicals

4,4-DDE d8, 4,4′-DDT d8, d4, β-HCH, δ-HCH, dicofol, dicofol d8, γ-HCH d6, hexaclorobenzene 13C, trifluralin d14, Pesticide-Mix 208, (100 μg mL^{-1}), PAHs-Mix 63, PAH-Mix 9 (deuterated) and PCB-Mix19 were purchased from Dr Ehrenstorfer (Augsburg, Germany). Labeled PCBs (#31, #52, #118, #153 and #194) were purchased from Wellington Laboratories (Ontario, Canada).

3.3.2. Sample extraction

The first step in the laboratory was the filtration of the water samples with 0.7 μm pore size glass fiber filters on a vacuum filter system for the extraction of the Suspended Sediments (SS). After filtration, each water sample resulted in 8 filters that were dried over silica gel in a desiccator until constant weight. The filters that constitute each sample were spiked with 15 μL of the surrogate solution at 1 ng g^{-1} and extracted by pressurized liquid extraction (PLE) using a Dionex ASE 350 accelerated solvent extractor (ASE) (Sunnyvale, CA, USA). The 22 mL ASE stainless steel cells were packed as follows: 2 g of Florisil powder was placed at the outflow side of the cell and 4 g more was added to the filter package. The remaining space was filled with Hydromatrix (Merck, Darmstadt, Germany) and before closing the cell a cellulose filter was placed at the bottom. A mixture of hexane:dichloromethane (1:1) was used as extraction solvent.

The simultaneous extraction and clean-up of the 42 analyzed compounds were briefly optimized according to previous studies that analyzed the same compounds in sediments and soils samples (Hildebrandt et al., 2009; Navarro-Ortega et al., 2010). Extracts were evaporated at room temperature to nearly dryness using a TurboVap LV from Caliper LifeSciences (Hopkinton, MA, USA) and reconstituted with hexane to a final volume of 100 μL into glass amber vials for gas chromatography.

3.3.3. Instrumental analysis

For PAHs, GC–MS analyses were carried out using a Trace 2000 gas chromatograph (Thermo Electron, USA) coupled to a mass spectrometer from Thermo Electron. In order to increase the sensibility and selectivity of organochlorine pollutants (DDX, PCBs and OCs), the analysis was performed using GC–MS/MS adapting the method described in Sanchís et al. (2013). A Trace GC-Ultra coupled to a triple quadrupole (QqQ) mass spectrometer TSQ Quantum (ThermoFischer Scientific) was employed. In both cases chromatographic separation was performed on a fused silica capillary column of 30 m × 0.25 mm I.D., and 0.25 μm film thickness, using helium as carrier gas (HP-5MS (J&W Scientific, Folsom, CA, USA) for PAHs and DB-5 MS (Agilent Technologies, CA, USA) for organochlorine pollutants). The mass spectrometer was operated in the electron ionization mode with an ionizing energy of 70 eV and the extracts were injected in the splitless mode. Oven temperatures were programmed following Navarro-Ortega et al. (2010). Although the presented multiresidue method is performed with only one extraction, the use of isotopic-labeled surrogates (16 labeled PAHs, 2 labeled DDX, 6 labeled PCBs and 4 labeled OCs) for the quantification of compounds and the control of method blanks guarantees a good quality of the analytical results. Data acquisition was carried out in the selected ion monitoring (SIM) mode. Each compound was separately quantified using a five-point calibration of mixed standard solutions in the range from 50 to 1000 mg L^{-1}. Method detection limits ranged respectively from 0.18 to 0.54 ng g^{-1} for PAHs, 0.002 to 0.025 ng g^{-1} for DDX, 0.001 to 0.0261 ng g^{-1} for PCBs and 0.001 to 0.005 ng g^{-1} for OCs (see Table S1 in Supporting Material).

3.4. Computation of pollutants' mass-flows and loads

Mass-flow m_{ij} (mg s^{-1}) for every single pollutant j at time t_i is calculated according to Eq. (1):

$$m_{ij} = Q_i \cdot SSC_i \cdot c_{ij} \cdot 10^{-6} \quad (1)$$

where Q_i is the river discharge in m^3s^{-1}, SSC_i is the suspended sediment in mg L^{-1}, c_{ij} is the concentration of pollutant j in ng g^{-1} and 10^{-6} is the appropriate unit conversion factor.

Total (cumulated) load of a given pollutant along the FF corresponds to the area under the mass-flow *vs* time curve (i.e., the integral curve). Thus, load of pollutant j corresponding to time interval comprised between t_i and t_{i+1} can be approximated by Eq. (2):

$$L_{ij} = \frac{(t_{i+1} - t_i) \cdot \left(m_{ij} + m_{(i+1)j}\right)}{2} \cdot 10^{-3} \quad (2)$$

where the load L_{ij} is expressed in g, the mass-flows m_{ij} and $m_{(i+1)j}$ in mg s^{-1}, the time interval in s and 10^{-3} is the corresponding conversion unit factor.

The total cumulated load of pollutant j along the flushing-flow event L_j (in g) is obtained by summation over all the time intervals:

$$L_j = \sum_{i=0}^{n} L_{ij} \quad (3)$$

4. Results and discussion

4.1. Flood hydrology and sediment load

Here, we summarize the general patterns of the hydrology and the suspended sediment load of the FFs in the lower Ebro, emphasizing the characteristics of the one performed in June 2012. The event monitored did not exactly resembled the habitual hydrograph implemented during the last years, but followed a new design elaborated to increase the effectiveness of the artificial releases on macrophyte removal, while minimizing the geomorphic effects of the clearwater releases. Peak flows registered at AMS during the event (i.e. 1284 m^3s^{-1} and 1323 m^3s^{-1}; Fig. 2) were remarkably higher that those performed following the ancient FF design (i.e. 1185 m^3s^{-1} and 1135 m^3s^{-1}). The peak discharge of the FF had a recurrence period of 1.6 year, estimated for the post-dam flow regime (1965–2012). Mean discharge during the event was 753 m^3 s^{-1} and ca. 40 hm^3 of water were released during the FF, a value that is in the same range than other studied events. However, the energy expenditure in the channel, expressed as the rate of discharge increment per unit time (Flashiness Index, FI, as per Batalla and Vericat, 2009) was higher in this event. Mean flood FIs obtained during FFs in the period 2002–2011 was 149 m^3s^{-1} h^{-1}; while in the present release the FI was 230 m^3s^{-1} h^{-1}, a fact that highlights the higher energy expenditure in the channel and thus the accordingly higher sediment transport. Suspended sediment concentration (SSC) and river flow discharge (Q) show a direct non-linear dependence (see Fig. S2, Supporting material) fitting a power type equation $SSC = 0.012 \cdot Q^{1.35}$ (eq. 4), which is consistent with previous observations (Batalla and Vericat, 2009).

Mean SSC at AMS during the FF was 155 mg L^{-1} ranging from a minimum of 40 mg L^{-1} to a maximum of 315 mg L^{-1} (Fig. 2). SSCs were higher than those observed in the same section during previous events that typically did not exceed 220 mg L^{-1}. Further downstream, SSC in PAMS was lower, ranging from a minimum of 4 mg L^{-1} to a maximum of 151 mg L^{-1} observed during the peak discharge. Values observed at PAMS were in the same order of magnitude than in previous FFs.

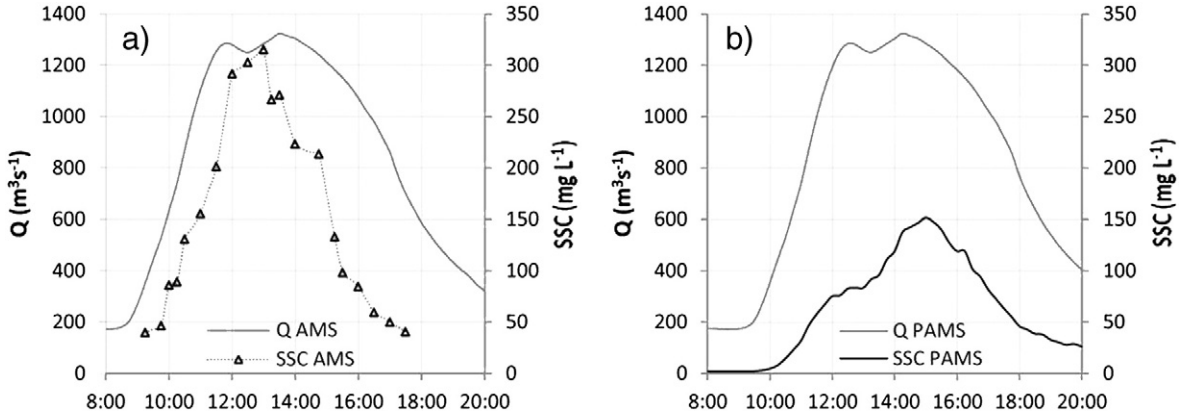

Fig. 2. Graphs showing river discharge (Q) and Suspended Sediment Concentration (SSC) profiles along time during the FF event at the locations AMS and PAMS respectively.

4.2. Occurrence of persistent organic pollutants

All the persistent organic pollutants analyzed in the present study show relatively high octanol–water partition constants (i.e., log $K_{ow} \geq 4$), the only exceptions being lightest PAHs and some HCH isomers (log K_{ow} 3.4 to 4). Therefore they are likely to be found in both steady sediments and particulate suspended material (it may be seen as a mobilized fraction of sediments) rather than in the aqueous phase in which they show a very low solubility. Only HCB and HCH are detectable in water, though the dissolved fraction was excluded from the present study, which is exclusively focused on transport of pollutants by particulate suspended material. Occurrence data of the various pollutants (mean, median, standard deviation, maximum, minimum, coefficient of variation and detection frequency) measured in suspended sediments during the FF event studied are reported in Table 1. Concerning PAHs, the overall concentration is around 100 ng g^{-1} which falls within the range described in the Ebro river for steady sediments (ca. 200 ng g^{-1}) (Hildebrandt et al., 2009). These PAHs concentrations are typical of rural environments rather than urban and industrial areas (Liu et al., 2012). This also applies to single constituents that are also consistent with sediment levels within a factor up to 2. Main differences are observed only for fluoranthene, chrysene and benzo(a)pyrene, the former two showing lower concentrations in particulate material (respectively 10 ng g^{-1} and 7.5 ng g^{-1} vs. 120 ng g^{-1} and 31.4 ng g^{-1} in sediments) while the latter shows the opposite trend (24 in particulate material and 6 ng g^{-1} in sediments). In fact, benzo(a)pyrene is the major constituent of the PAHs mixture (24% on average), followed by phenanthrene (19%) and fluoranthene (11%). Mixture profile is consistent with a pyrolytic (combustion) origin (indexes IP/276 and BaA/228 ca. 0.35 and 0.34 respectively) (Arias et al., 2010). Furthermore, predominance of less volatile compounds in the mixture would be indicative of local pollution influence rather than long range atmospheric transport (Fernández and Grimalt, 2003). Generally, PAH compounds exhibited fairly constant concentrations during the FF, which are reflected in individual low to moderate standard deviations and coefficients of variation (CV) (20% to 64%). Total PAHs ranged from 76 to 146 ng g^{-1} with a CV of 21.5%. These results indicate that there is a low connection between these compounds and the studied FF. The concentrations of PAHs found in the particulate are likely due to diffuse pollution rather than to the mobilization of the contaminated sediments.

Even though DDT and PBCs are banned since long time and their former production in Flix discontinued, the presence of contaminated sediments constitutes a known source for these compounds downstream in the Ebro. As mentioned before, one of the specific objectives of the present study is to characterize their mobilization and transport patterns. DDT and its transformation compounds DDE and DDD are fully detectable in particulate material, in good concordance with previously data reported in the same location for steady sediments. The average values are comprised between 0.92 and 187 ng g^{-1}, the latter corresponding to 4,4′-DDT. These values are slightly higher than those reported for steady sediments of the same river section in the last 10 years: 11 to 63.5 ng g^{-1}(Navarro et al., 2006), 4 to 30 ng g^{-1} (Lacorte et al., 2006) and 3 to 48 ng g^{-1}(Navarro-Ortega et al., 2010) indicating as a probable source the polluted sediments located in Flix industrial complex. Peak values of 4,4′-DDT up to 1400 ng g^{-1} are notwithstanding, being the main contributor to this family of compounds (75% on average). Such a high value of the parent compound point to recent illegal releases in concordance with the existing literature (Lacorte et al., 2006; Gómez-Gutiérrez et al., 2007; Bosch et al., 2009).

Measured concentration ranges for PCBs in particulate suspended material (13 to 1445 ng g^{-1}) are fairly coincident with those already described for steady sediments in this reach of the Ebro river (Fernández et al., 1999), being again their most likely source the polluted pack of sediments located in Flix industrial complex, in which they were formerly manufactured. Major PCB constituents are the less volatile congeners 170, 180 and 194 with average levels and contributions of 88 ng g^{-1} (26%), 157 ng g^{-1} (46%) and 61 ng g^{-1} (18%) respectively.

Other OCs are largely dominated by HCB (95% contribution on average), a known by-product generated in the chloro-alkali industry located nearby upstream (Flix) and in less extent to HCH, being among them isomers β and γ (lindane) the most relevant. δ-HCH isomer as well as aldrin are detected in trace amounts while α HCH, and dicofol are below the limit of detection. Range levels for HCB are in agreement with those described in the literature for sediments (Navarro-Ortega et al., 2010), being the maximum somewhat higher, which is consistent with the proximity of the Flix hot-spot.

In sharp contrast with PAHs, range levels of all organochlorine pollutants (OCs, DDX and PCBs) detected in suspended particulate material show a high variation along the period observed (CV% usually higher than 100%). That fact can be interpreted in terms of the characteristics of the pollution sources involved, as deeply explained in Section 4.3. While PAHs show a diffuse source not influenced by the FF, the rest of compounds present in the contaminated sediments of the Flix dam have been mobilized downstream during the FF together with the sediments.

4.3. Mass-flows and load budgets

Floods, including both natural and FFs, are the main responsible of sediment transport in rivers. In the case of rivers regulated by dams the total load transported during natural floods is usually much higher than during artificial floods, mainly due to their larger peaks and duration (Batalla and Vericat, 2009). However, in dry years, and in the

Table 1
Mean, median, standard deviation, maximum, minimum concentrations (ng g^{-1}), coefficient of variation and detection frequency of pollutants measured in suspended solids during the FF and reference regulatory values (see text).

Compounds	Mean (ng g^{-1})	Median (ng g^{-1})	Std. Dev. (ng g^{-1})	Max (ng g^{-1})	Min (ng g^{-1})	C.V. %	D.F. %	ISQC (ng g^{-1})	TEC (ng g^{-1})	PEC (ng g^{-1})	RCRA (ng g^{-1})
PAHs											
Naphthalene	bld	bld	bld	bld	bld	–	0	34.6	176	561	–
Acenaphthylene	bld	bld	bld	bld	bld	–	0	5.87	5.9	128	–
Acenaphthene	2.774	2.684	1.287	5.627	1.247	46.4	100	6.71	6.71	89	–
Fluorene	4.951	4.161	2.490	10.835	2.431	50.3	92.3	21.2	77.4	536	–
Phenanthrene	18.878	19.024	5.148	26.845	12.153	27.3	100.0	41.9	204	1170	–
Anthracene	0.526	0.471	0.336	1.129	0.042	63.9	92.3	46.9	57.2	845	–
Fluoranthene	10.784	10.040	3.061	15.986	6.175	28.4	100	111	423	2230	–
Pyrene	9.610	9.081	2.525	14.546	6.178	26.3	100	53	195	1520	–
Benzo(a)anthracene	3.731	3.691	0.933	5.449	1.981	25.0	100	31.7	108	1050	–
Crysene	7.478	7.254	1.686	10.600	4.691	22.5	92.3	57.1	166	1290	–
Benzo(b)Fluoranthene	6.862	7.003	1.528	9.231	4.612	22.3	100	–	240	13,400	–
Benzo(k)fluoranthene	4.946	5.001	0.977	6.215	3.817	19.8	69.2	–	240	13,400	–
Benzo(a)pyrene	24.159	21.986	8.714	43.844	13.713	36.1	100	31.9	150	1450	–
Indenoe(1.2.3-c.d)pyrene	3.672	3.920	0.949	4.472	2.624	25.8	23.1	–	200	3200	–
Dibenzo(a.h)anthracene	bld	bld	bld	bld	bld	–	0	6.22	33	135	–
Benzo(g.h.i)perylene	7.373	7.118	1.496	9.531	5.217	20.3	92.3	–	170	3200	–
∑ PAHs	99.8	97.1	21.5	146.4	75.6	21.5	100				
Organochlorines											
HCB	64.661	3.363	129.788	435.958	0.817	200.7	100	–	–	–	20
α-HCH	bld	bld	bld	bld	bld	–	0	–	6	100	–
β-HCH	1.114	1.327	0.643	2.182	0.178	57.7	100	–	5	210	–
γ-HCH (Lindane)	1.794	1.489	1.141	5.203	0.937	63.6	100	0.94	2.37	4.99	–
δ-HCH	0.058	0.083	0.063	0.218	0.024	109.0	58.3	–	–	–	–
Aldrin	0.059	0.063	0.065	0.222	bld	110.0	66.7	–	2	80	–
Dicofol	bld	bld	bld	bld	bld	–	–	–	–	–	–
∑ OC	67.7	6.5	130.0	440.1	3.7	192.0	100				
DDX											
2.4-DDE	12.292	6.826	16.035	60.975	3.179	141.3	100	Σ = 1.42[a]	Σ = 3.2[a]	Σ = 31.3[a]	–
4.4′-DDD	12.032	1.617	26.307	95.674	0.533	236.9	100	Σ = 3.54[b]	Σ = 4.9[b]	Σ = 28.0[b]	–
2.4′-DDT	0.918	0.347	1.344	4.885	bld	158.6	91.7	Σ = 1.19[c]	Σ = 4.2[c]	Σ = 62.9[c]	–
2.4′-DDD	8.039	4.158	9.661	33.169	1.611	120.2	100	–[b]	–[b]	–[b]	–
4.4′-DDE	17.830	7.487	22.691	68.890	2.405	127.3	100	–[a]	–[a]	–[a]	–
4.4′-DDT	187.219	30.142	418.910	1467.047	5.810	223.8	100	–[c]	–[c]	–[c]	–
∑ DDX	238.3	48.8	472.5	1651.7	19.3	198.3	100	–	5	572	–
PCB											
PCB 18	0.513	0.246	0.744	2.703	0.087	145.0	100	–	–	–	–
PCB28(3) + PCB31	0.203	0.172	0.115	0.466	0.091	56.7	100	–	–	–	–
PCB44	0.717	0.401	0.682	2.484	0.102	95.2	100	–	–	–	–
PCB52	1.102	0.668	1.227	3.729	0.035	111.3	100	–	–	–	–
PCB 101	16.671	8.393	18.289	56.503	4.734	109.7	100	–	–	–	–
PCB 118	2.012	1.988	1.698	5.140	0.600	84.4	77.8	–	–	–	–
PCB 138	2.611	1.679	2.981	11.320	0.483	114.2	100	–	–	–	–
PCB 153	6.884	4.413	5.664	19.065	1.926	82.3	100	–	–	–	–
PCB 170	87.858	2.407	151.006	415.638	0.733	171.9	66.7	–	–	–	–
PCB 180	157.079	8.310	262.031	687.324	1.273	166.8	100	–	–	–	–
PCB 194	60.872	7.149	93.898	233.049	1.231	154.3	100	–	–	–	–
PCB 149	5.571	3.569	4.569	15.815	1.721	82.0	100	–	–	–	–
∑ PCB	342.1	38.9	538.5	1445.6	13.1	157.4	100	34.1	59.8	676.0	–

bld: below limit of detection.
[a] Sum of 2.4′-DDE and 4.4′-DDE.
[b] Sum of 2.4′-DDD and 4.4′-DDD.
[c] Sum of 2.4′-DDT and 4.4′-DDT.

absence of natural floods, the contribution of FFs to the annual load may become remarkable. The sediment load estimated during the June 2012 FF in the River Ebro varies between the two monitoring sections. The suspended sediment load estimated at AMS by means of direct sampling attained 5766 T (i.e. from 9:00 am to 6:00 pm) while at PAMS was at around 3010 T for the same period of time. This last value fits with the mean value observed for all the other previous FFs (mean of 3040 T, with a standard deviation of 1512 T); in contrast, the estimated load at AMS was the largest ever registered.

Sediment dynamics in regulated rivers, thus sediment supply-limited systems, are rather complex and not only function of the hydrology. In the lower Ebro several parameters such as antecedent conditions, sediment availability exhaustion, flashiness, loss of energy due to flow routing and overflooding have been discussed to play an important role in sediment dynamics (Tena et al., 2012a). Within this context, the difference observed in the sediment load of the studied sections could be attributed to any of the previous parameters or a combination of them. In this case, even there is a short distance between the two sections (e.g. 4 km), sharp changes in channel width or depth, water velocity, as well as the distance from the Flix Dam influences directly the sediment dynamics. For instance, sediment resuspension due to energy expenditure in the channel is higher in the upstream section (i.e. AMS); while such resuspension could turn into deposition in the downstream section due to the energy loss, thus increasing the sediment storage in this reach and reducing the sediment transported in PAMS.

Concerning the contaminants, mass-flows (mg s^{-1}), as well as total loads (i.e., cumulated loads expressed in g) transported by suspended sediments along the FF time period for the different specific compounds and families analyzed were calculated as described in Section 3.4. Results are summarized in Table S2 (Supporting material). Observed average mass-flow of PAHs along the flushing-flow event was about 20 mg s^{-1}, with a maximum of 34 mg s^{-1} coincident with that of SSC. Such a low variation in PAHs mass flows (CV = 42%) indicates homogeneity of the pollution source, which is consistent with a local diffuse pollution related to combustion processes. Owing to this, total PAHs mass-flow ($m_{\Sigma PAH}$) shows a more linear correlation with suspended solids (expressed either as SSC or turbidity) than with discharge Q. While both fit a power equation $Y = A \cdot X^{\alpha}$, the exponents α characterizing the dependence of PAH mass-flow ($Y = m_{\Sigma PAH}$) on discharge (X = Q) and suspended solids (X = NTU, SSC) are 2.6 and 1.65 respectively, the latter clearly closer to unity. Similar to what is observed in the concentration pattern, the minimum and the maximum mass-flow during the FF for the rest of compounds differ significantly, especially for HCB, 4,4′-DDT and the heavier PCBs indicating high dependence with the FF.

Fig. 3a to d shows the evolution of mass-flows (mg s^{-1}) along time, as well as the cumulated load (i.e., their integral curve, g) for the four families of compounds. The observed profile is consistent with the results previously shown. PAHs show a variable mass-flow over the period of time evaluated with no clear tendency and no correlation between the maximum mass-flow and the maximum Q (Fig. 3a). Consequently, total load grows steadily along time, reaching at the end of the monitoring period a value of ca. 403 g.

Remarkably, organochlorine pollutants (DDX, PCBs and OCs) show a totally different pattern behavior, characterized by sharp peaks relatively early on time (at ca. 1 h 15 min) followed by a rapid subsequent decay. Thus, for instance, OCs have a maximum mass-flow of 66.1 mg s^{-1} with an average of 8.2 mg s^{-1}; DDX 247.9 and 38.2 mg s^{-1} and PCBs 217 and 44.8 mg s^{-1}, respectively. Such a high ranges of variability are well reflected on CVs of 150–200%. Consequently, cumulative load curves grow up very quickly (Fig. 3b–d).

For comparative purposes, we also provide an estimation of what can be called *basal loads* (Fig. 3a to d), calculated using the average river discharge recorded in the period 1912–2012 (436 m^3 s^{-1}), a corresponding basal SSC value of 36.6 mg L^{-1} obtained using Eq. (4) (Section 4.1.), the same time interval of the period surveyed (19,800 s) and the average concentration level of each family measured in this study (Table 1). Basal values found for the four families are represented in Fig. 3a to d. Cumulated basal loads for the various families are respectively PAHs, 31 g; OCs, 21.5 g; DDX, 75.3 g and PCBs, 108.1 g. Comparing these load values with the actual ones measured during the event, i.e., PAHs, 403 g; OCs, 207.5 g; DDX, 940.5 g and PCBs, 1038.9 g; this indicates that even though the peak discharge reached during the FF merely exceeds the basal flow by a factor of 3 (436 vs. 1300 m^3 s^{-1}) the transport of contaminants is increased by a factor up to 10 to 13.

A final warning remark about load budgets as presented in this study is necessary: it must be kept in mind that the given figures are conservative since they only take into account the fraction of pollutants adsorbed on suspended sediment without accounting for the dissolved fraction. Whereas for the majority of pollutants this fraction is expected to be negligible due to the very low water solubility of the concerned compounds, this is not the case of few of them, such as HCH isomers, HCB and the lightest PAHs (naphthalene, acenaphthene, acenaphthylene, fluorene, phenanthrene) whose solubility in water is perceptible.

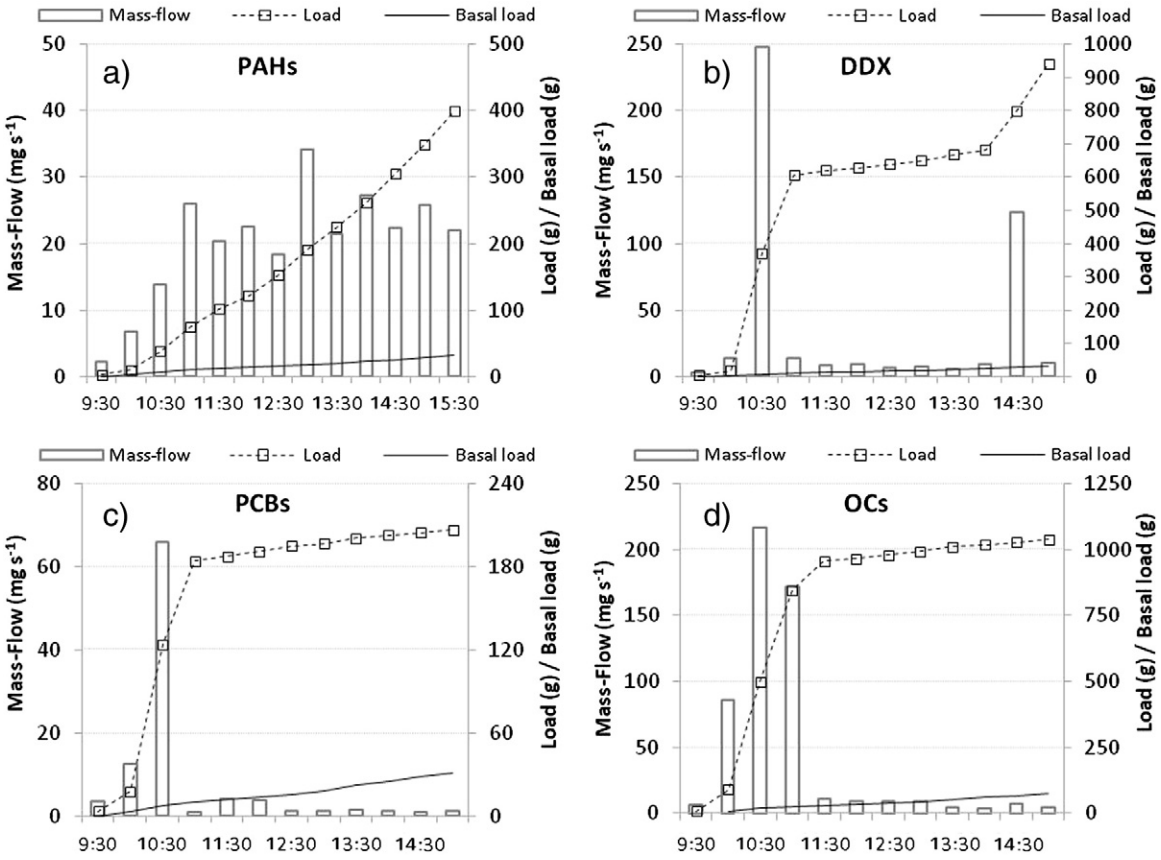

Fig. 3. Graphs showing mass-flows, actual and basal cumulated loads transported by the river along time during the FF event for the different pollutants' families (a) PAHs; (b) DDX; (c) PCBs and (d) OCs.

4.4. Regulatory assessment

The concentrations obtained were also compared with some legislated limits in sediments assuming that the majority of the SS obtained come from the resuspension of sediments due to increasing energy during the flash-flow event and that pollutants in SS coming from air pollution is in comparison insignificant in this case. In this way, three different guidelines that specially address sediment management were considered: The Interim freshwater Sediment Quality Guidelines (ISQC) (Canadian Council of Ministers of the Environment, 2002); the Threshold Effect Concentration (TEC; below which adverse effect are not expected to occur) and the Probable Effect Concentration (PEC, above which adverse effects are expected to occur more often than not), both from MacDonald et al. (2000); and the guideline defined by the Resource Conservation and Recovery Act (RCRA, USEPA, 1976).

As far as EU legislation is concerned, Directive 2013/39/UE (European Council, 2013) (an extension of the Water Framework Directive) explicitly sets annual average and maximum allowable concentration Environmental Quality Standards (respectively referred to as AA-EQS and MAC-EQS) in surface waters, while EQS for sediments and biota are generally left to the provisions of member states. Thus, recalculating particulate concentration (ng g^{-1}) values to concentrations in water (ng L^{-1}) obtained in the present study we found that HCB exceeds the MAC-EQS (59.9 vs 50 ng L^{-1}) while DDX (sum of DDT, DDE and DDD) and 4,4′DDT exceed the AA-EQSs set by the above referred Directive (respectively 33.6 and 26.1 ng L^{-1} mean concentrations in water compared to AA-EQSs of 25 and 10 ng L^{-1}).

Among the PAH compounds analyzed, benzo(a)pyrene presented a maximum concentration of 43.8 ng g^{-1} (Table 1 and Fig. 4a), which is slightly above the most restrictive limit (ISQC, 31.7 ng g^{-1}). Special attention has to be paid to this compound considered as one of the most carcinogenic among PAHs. In the case of organochlorine pollutants an important contribution of the DDX (DDT, DDE and DDD) is observed (Table 1 and Fig. 4b), especially 4,4′-DDT, although this compound is forbidden in the EU (and thus in Spain) for agricultural purposes since 1977. Samples showed DDX maximum concentration (1651 ng g^{-1}) above the PEC limits (572 ng g^{-1}) and mean concentrations (238.3 ng g^{-1}) between the TEC and the PEC limit. The minimum DDX concentration found during the FF, 19.3 ng g^{-1}, also exceeds the TEC, resulting in a high potential risk for the living organisms in the river ecosystem in steady conditions which is increased dramatically during FF. Similarly, the sum of all PCBs analyzed, which maximum sum concentration (1445.6 ng g^{-1}) exceeds by far the PEC limit (676 ng g^{-1}) and with a mean concentration between the TEC (59.8 ng g^{-1}) and the PEC limits. Both the maximum and the mean concentration of PCBs also exceed the ISQC established at 34.1 ng g^{-1}. In this case the minimum PCB concentration found is underneath the three thresholds considered and consequently the potential risk for the living organisms is a direct consequence of the FF and its remobilization of the contaminated sediments accumulated in the Flix dam.

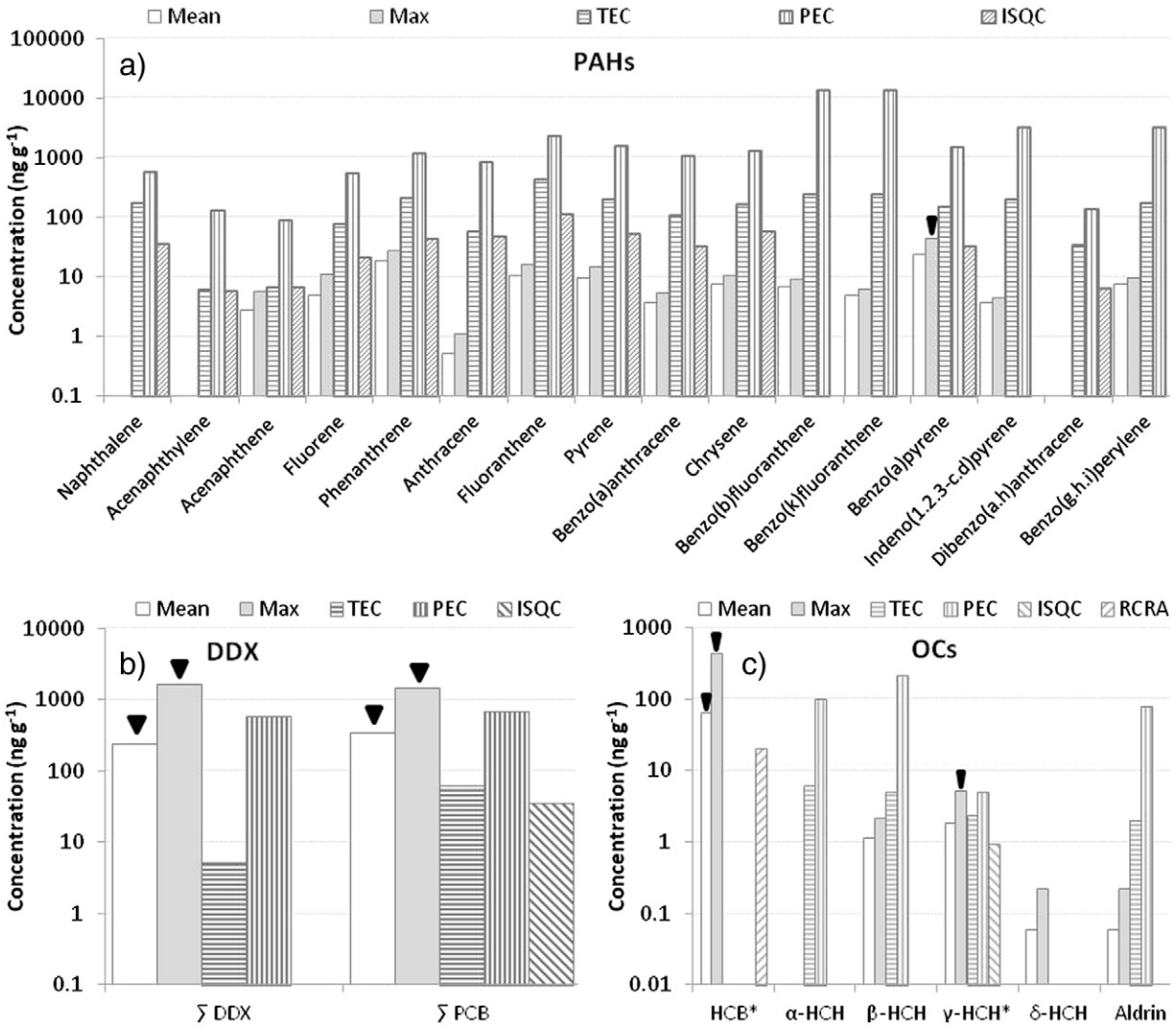

Fig. 4. Measured mean and maximum concentrations of different compounds analyzed on particulate material compared to some reference and regulatory values (see text). Values identified with an inverted black triangle (▼) indicate noncompliance with any reference regulatory levels. (a) PAHs; (b) DDX and PCBs; (c) OCs.

Other compounds detected at concentrations exceeding regulatory references are (Table 1 and Fig. 4c): HCB, with maximum concentration (435,96 ng g^{-1}) and mean concentration (64.7 ng g^{-1}) far above the RCRA limits (20 ng g^{-1}) and γ-HCH, with maximum concentration (5.2 ng g^{-1}) above the PEC limit (4.99 ng g^{-1}) and mean concentration (1.79 ng g^{-1}) between the TEC (2.37 ng g^{-1}) and the PEC limit. In both cases the minimum concentration found is underneath the thresholds indicating the same behavior than the previously explained for PCBs.

5. Conclusions

Programmed FFs allow studying both quantitatively and qualitatively how polluted sediments are transported under controlled conditions. The main conclusions of this research can be drawn as follows:

(i) The suspended sediment load estimated at the monitoring sections was, on average, 4400 tones (for a total runoff of 40 hm^3). This load is in the range of those observed in previous FFs (i.e. performed since 2002 in this river). Overall, suspended sediment concentrations were slightly higher than those measured in previous releases, a fact that may be a response to the new hydrograph design that enhances energy expenditure in the channel,

(ii) Concentration of some relevant pollutants found in the suspended sediments, such as HCB, DDT and PCBs, largely exceeded existing reference regulatory values established for sediments.

(iii) Evolution of concentrations, mass-flows and total cumulated load budgets along time was estimated and compared to a *basal* or average scenario. Our estimations show that transport of pollutants mostly occurs under high flow conditions.

The remarkable mobilization of pollutants during flood flows should be taken into consideration for the future management of contaminated rivers, especially those located downstream from dams, from which periodical water releases are performed. This is particularly important in Mediterranean Rivers, for which this hydrological behavior is consubstantial to the precipitation regime.

Supplementary data to this article can be found online at http://dx.doi.org/10.1016/j.scitotenv.2013.11.040.

Acknowledgments

This work was supported by the Spanish Ministry of Economy and Competitiveness through the Consolider-Ingenio 2010 project SCARCE (CSD2009-00065) and by the Generalitat de Catalunya (Consolidated Research Group: Water and Soil Quality Unit 2009-SGR-965). The research leading to these results has received funding from the European Comunities 7th Framework Programme under Grant Agreement No. 603629-ENV-2013-6.2.1-Globaqua.

References

Amaral OC, Otero R, Grimalt JO, Albaigès J. Volatile and semi-volatile organochlorine compounds in tap and riverine waters in the area of influence of a chlorinated organic solvent factory. Water Res 1996;30:1876–84.

Arias AH, Vazquez-Botello A, Tombesi N, Ponce-Vélez G, Freije H, Marcovecchio J. Presence, distribution, and origins of polycyclic aromatic hydrocarbons (PAHs) in sediments from Bahía Blanca estuary, Argentina. Environ Monit Assess 2010;160:301–14.

Batalla RJ, Vericat D. Hydrological and sediment transport dynamics of flushing flows: implications for management in large Mediterranean rivers. River Res Appl 2009;25:297–314.

Batalla RJ, Sala M, Werritty A. Sediment budget focused in solid material transport in a subhumid Mediterranean drainage-basin. Z Geomorphol 1995;39:249–64.

Batalla RJ, Gómez CM, Kondolf GM. Reservoir-induced hydrological changes in the Ebro River basin (NE Spain). J Hydrol 2004;290:117–36.

Bosch C, Olivares A, Faria M, Navas JM, del Olmo I, Grimalt JO, Piña B, Barata C. Identification of water soluble and particle bound compounds causing sublethal toxic effects. A field study on sediments affected by a chlor-alkali industry. Aquat Toxicol 2009;94:16–27.

Brookes A. River channel restoration: theory and practice. Changing river channels. Chichester: Wiley & Sons; 1995.

Canadian Council of Ministers of the Environment. Canadian sediment quality guidelines for the protection of aquatic life. Winnipeg: Canadian Council of Ministers of the Environment; 2002.

Carrizo D, Grimalt JO. Rapid and simplified method for the analysis of polychloronaphthalene congener distributions in environmental and human samples by gas chromatography coupled to negative ion chemical ionization mass spectrometry. J Chromatogr A 2006;1118:271–7.

CHE. Confederación Hidrográfica del Ebro. Retrieved July 2012, fromhttp://www.chebro.es, 2012.

Downs PW, Kondolf GM, Skinner KS. Rivers and streams. In: Davy A, Perrow M, editors. Handbook of ecological restoration. New York: Cambridge University Press; 2002. [Restoration in practice: 267–296].

European Council. Directive 2013/39/EC of the European Parliament and of the council of 12 August 2013 amending directives 200/30/EC and 2008/105/EC as regards priority substances in the field of water policy; 2013.

Fernández P, Grimalt JO. On the global distribution of persistent organic pollutants. Chimia 2003;57:514–21.

Fernández MA, Alonso C, González MJ, Hernández LM. Occurrence of organochlorine insecticides, PCBs and PCB congeners in waters and sediments of the Ebro River (Spain). Chemosphere 1999;38:33–43.

Garcia C, Laronne JB, Sala M. Continuous monitoring of bedload flux in a mountain gravel-bed river. Geomorphology 2000;34:23–31.

Gómez-Gutiérrez AI, Jover E, Bodineau L, Albaigés J, Bayona JM. Organic contaminant loads into the Western Mediterranean Sea: estimate of Ebro River inputs. Chemosphere 2006;65:224–36.

Gómez-Gutiérrez A, Garnacho E, Bayona JM, Albaigés J. Assessment of the Mediterranean sediments contamination by persistent organic pollutants. Environ Pollut 2007;148:396–408.

Hildebrandt A, Lacorte S, Barceló D. Occurrence and fate of organochlorinated pesticides and PAH in agricultural soils from the Ebro River Basin. Arch Environ Contam Toxicol 2009;57:247–55.

Kondolf GM, Wilcock PR. The flushing flow problem: defining and evaluating objectives. Water Resour Res 1996;32:2589–99.

Lacorte S, Raldúa D, Martínez E, Navarro A, Diez S, Bayona JM, et al. Pilot survey of a broad range of priority pollutants in sediment and fish from the Ebro river basin (NE Spain). Environ Pollut 2006;140:471–82.

Lehner B, Doll P, Alcamo J, Henrichs T, Kaspar F. Estimating the impact of global change on flood and drought risks in Europe: a continental, integrated analysis. Clim Change 2006;75:273–99.

Liu Y, Beckingham B, Ruegner H, Li Z, Ma L, Schwientek M, et al. Comparison of sedimentary PAHs in the rivers of Ammer (Germany) and Liangtan (China): differences between early- and newly-industrialized countries. Environ Sci Technol 2012;47:701–9.

MacDonald DD, Ingersoll CG, Berger TA. Development and evaluation of consensus-based sediment quality guidelines for freshwater ecosystems. Arch Environ Contam Toxicol 2000;39:20–31.

Milhous RT. Effect of sediment transport and flow regulation on the ecology of gravel-bed rivers. Gravel-bed rivers. Chichester: Wiley & Sons; 1982.

Navarro A, Tauler R, Lacorte S, Barceló D. Chemometrical investigation of the presence and distribution of organochlorine and polyaromatic compounds in sediments of the Ebro River Basin. Anal Bioanal Chem 2006;385:1020–30.

Navarro-Ortega A, Tauler R, Lacorte S, Barceló D. Occurrence and transport of PAHs, pesticides and alkylphenols in sediment samples along the Ebro River Basin. J Hydrol 2010;383:5–17.

Novoa M. Precipitaciones y avenidas extraordinarias en Catalunya. Proceedings of the Jornadas de Trabajo sobre Inestabilidad de laderas en el Pirineo, Barcelona; 1984.

Olivares A, Quirós L, Pelayo S, Navarro A, Bosch C, Grimalt JO, et al. Integrated biological and chemical analysis of organochlorine compound pollution and of its biological effects in a riverine system downstream the discharge point. Sci Total Environ 2010;408:5592–9.

Prats J, Armengol J, Marcé R, Sánchez-Juny M, Dolz J. Dams and reservoirs in the lower Ebro River and its effects on the river thermal cycle. In: Barceló D, Petrovic M, editors. The Ebro River Basin. Springer Berlin Heidelberg; 2011. p. 77–95.

Reiser DW, Wesche TA, Estes C. Status of instream flow legislation and practices in North America. Fisheries 1989;14:22–9.

Rügner H, Schwientek M, Beckingham B, Kuch B, Grathwohl P. Turbidity as a proxy for total suspended solids (TSS) and particle facilitated pollutant transport in catchments. Environ Earth Sci 2013;69:373–80.

Sabater S, Artigas J, Gaudes A, Muñoz I, Urrea G, Romaní AM. Long-term moderate nutrient inputs enhance autotrophy in a forested Mediterranean stream. Freshw Biol 2011;56:1266–80.

SAIH. Ebro (automatic hydrological information system of the Ebro Basin). http://195.55.247.237/saihebro/index.php. [Visited 28th June 2012. 2012].

Sanchís J, Martínez E, Ginebreda A, Farré M, Barceló D. Occurrence of linear and cyclic volatile methylsiloxanes in wastewater, surface water and sediments from Catalonia. Sci Total Environ 2013;443:530–8.

Schwientek M, Rügner H, Beckingham B, Kuch B, Grathwohl P. Integrated monitoring of particle associated transport of PAHs in contrasting catchments. Environl Pollution 2013;172:155–62.

Soto DX, Roig R, Gacia E, Catalan J. Differential accumulation of mercury and other trace metals in the food web components of a reservoir impacted by a chlor-alkali plant

(Flix, Ebro River, Spain): Implications for biomonitoring. Environ Pollut 2011;159: 1481–9.
Tena A, Batalla RJ. The sediment budget of a large river regulated by dams (the lower River Ebro, NE Spain). J Soils Sediments 2013;13:966–80.
Tena A, Batalla RJ, Vericat D, López-Tarazón JA. Suspended sediment dynamics in a large regulated river over a 10-year period (the lower Ebro, NE Iberian Peninsula). Geomorphology 2011;125:73–84.
Tena A, Batalla RJ, Vericat D. Reach-scale suspended sediment balance downstream from dams in a large Mediterranean river. Hydrol Sci J 2012a;57:831–49.
Tena A, Ksiazek L, Vericat D, Batalla RJ. Assessing the geomorphic effects of a flushing flow in a large regulated river. River research and applications; 2012b.
USEPA. Region 5, resource conservation and recovery act, ecological screening levels, 2003; 1976.
Vericat D, Batalla RJ. Sediment transport in a large impounded river: the lower Ebro, NE Iberian Peninsula. Geomorphology 2006;79:72–92.
Vericat D, Batalla RJ. Sediment transport from continuous monitoring in a perennial Mediterranean stream. Catena 2010;82:77–86.